Available online at www.sciencedirect.com
ScienceDirect
Journal of Molecular Catalysis A: Chemical 270 (2007) 132–143
JOURNAL OF MOLECULAR CATALYSIS A: CHEMICAL
www.elsevier.com/locate/molcata

Ru- and Fe-based *N*,*N*′-bis(2-pyridylmethyl)-*N*-methyl-(1*S*,2*S*)-1,2-cyclohexanediamine complexes immobilised on mesoporous MCM-41: Synthesis, characterization and catalytic applications

Tamijselvy Soundiressane [a], S. Selvakumar [b], Stéphane Ménage [a], Olivier Hamelin [a], Marc Fontecave [a], Anand P. Singh [b,*]

[a] *Laboratoire de Chimie et Biochimie des Centres Redox Biologiques, CEA, DSV-DRDC, CNRS UMR 5047, Université Joseph Fourier, 17 rue des Martyrs, 38054 Grenoble Cedex, France*
[b] *Catalysis Division, National Chemical Laboratory, Pune 411 008, India*

Received 29 August 2006; received in revised form 15 January 2007; accepted 21 January 2007
Available online 24 January 2007

Abstract

Protected mesoporous MCM-41 phases were synthesized by grafting of the ligand, (1*S*,2*S*)-*N*,*N*′-bis-pyridin-2-ylmethyl-cyclohexane-1,2-diamine (L_2Me), through the reactive 3-chloropropyltrimethoxysilane (3-CPTMS) group and designated as L_2Me-MCM-41. Subsequently, $RuCl_3$ and $Fe(BF_4)_2$ or $Fe(CF_3SO_3)_2$ were added to the heterogenized L_2Me-MCM-41 for complexation and designated as M-L_2Me-MCM-41 (M = Ru and Fe). All samples were characterized in detail using XRD, N_2 sorption isotherm, FT-IR, TGA-DTA, XPS, UV–vis, solid state ^{13}C NMR, EPR and elemental analysis, etc. The XRD and sorption measurements of the catalyst confirmed the structural integrity of the mesoporous hosts and the spectroscopic characterization techniques proved the successful anchoring of the metal complexes over the modified mesoporous support. The screening of catalyst M-L_2Me-MCM-41 was done for the oxidation reaction of thioanisole (methyl phenyl sulphide) using H_2O_2 as an oxidant. The Ru-L_2Me-MCM-41 and Fe-L_2Me-MCM-41 catalysts show higher activities and turnover numbers and exhibit enantiomeric excess comparable to the homogeneous catalysts, Ru-$L_2(Me)_2$ and Fe-$L_2(Me)_2$. Furthermore, Fe-L_2Me-MCM-41 and Fe-$L_2(Me)_2$ were also found active in the epoxidation of styrene. These results indicate that metal complexes are confined into the pore of the material which play a major role in the reaction.

Keywords: Heterogenization; M-L_2Me-MCM-41; Metal complexes; Sulfoxidation

1. Introduction

Immobilization of catalysts on inorganic matrices has been a great area of research for academic and industrial points of view, as this method affords an ideal combination of the advantages of homogeneous catalysts and avoids their disadvantages related to handling and reusability of the catalyst [1]. In this field, only few iron complexes have been designed for heterogeneous catalysts for oxidation catalysis [2], whereas Mn salen and metalloporphyrins have been widely studied [3]. The emergence of new non-heme iron catalysts for alkanes, alkenes and sulfides oxidation by H_2O_2 during the recent years prompted us to graft tetradentate pyridine/amine ligands, derivated from BISPICEN ligand (BISPICEN = *N*,*N*'-bis(2-pyridylmethyl)-1,2-ethanediamine) into a mesoporous phase [4]. Among them, a few have been found enantioselective for transformations of alkenes into epoxides and *cis*-diols [5] and sulfides into sulfoxides [6]. Their main interest reside into their easy accessibility even though their enantioselectivity was moderate in most cases and suffer of a lack of stability.

After the discovery of M41S family of mesoporous silicates and aluminosilicate materials by Mobil scientists in 1992 [7,8], MCM-41 has become the most popular member of the group due to their unique textural features and simple synthesis procedures. The most interesting feature of MCM-41 is its regular pore system, which consists of a hexagonal array of unidimensional,

* Corresponding author. Tel.: +91 20 2590 2497; fax: +91 20 2590 2633.
E-mail address: ap.singh@ncl.res.in (A.P. Singh).

1381-1169/$ – see front matter © 2007 Elsevier B.V. All rights reserved.
doi:10.1016/j.molcata.2007.01.037

hexagonally shaped pores. The pore diameter of MCM-41 can be varied systematically between 2 and 10 nm by use of surfactants with different chain lengths and pore expanders like trimethyl benzene (TMB). The catalytic properties of the MCM-41 materials can be adjusted by the incorporation of different metals into the MCM-41 framework [9–11]. Further, the diversity in the catalytic properties can be broadened by the grafting of organosilanes which contain organic functional groups onto the internal pore surfaces [12–14] or incorporating them during the synthesis process. An advantage of there organic–inorganic hybrid mesoporous materials is that they do not swell or dissolve in organic solvents and they have other advantages such as their superior mechanical and thermal stabilities [15–17]. Moreover, the leaching of active sites can also be avoided as the organic moieties are covalently attached to inorganic supports.

Accordingly, we report on this paper our attempt to graft Fe and Ru metal complexes of *N*,*N*′-bis(2-pyridylmethyl)-*N*-methyl-(1*S*,2*S*)-1,2-cyclohexanediamine (L_2Me), a version of the BISPICEN ligand, and some of its derivatives into MCM-41 phases and their catalytic properties for sulfides oxidations by H_2O_2. The immediate goals of our study were (i) to evaluate the heterogenisation method of the L_2Me ligand over mesoporous MCM-41 support, (ii) the effect of the support on the conversion and oxidation of methyl phenyl sulfide by hydrogen peroxide and (iii) to determine the extent of the increased stability of the catalysts with regard to the homogeneous catalysts as well as their recycling properties.

2. Experimental

2.1. Synthesis of parent and organo-functionalized MCM-41

The Si-MCM-41 was prepared from the gel with the following composition—SiO_2:CTMABr:NaOH:H_2O 1: 0.19:0.4:78. In a typical synthesis, cetyltrimethylammonium bromide (CTMABr) was added to the solution of NaOH in H_2O, under stirring and the mixture was further stirred for 1 h. To this mixture, calculated amount of fumed silica was added slowly. The gel mixture was stirred for 6 h and pH was adjusted to 10.7–10.9 by addition of 0.1 M HCl solution. Finally the mixture was transferred into a Teflon-lined autoclave and kept at 100 °C under static conditions for 72 h. The solid material obtained was then filtered, washed well with distilled water till the filtrate shows a neutral pH, and then air-dried. The surfactant of the as-synthesized mesoporous sample was removed by calcination in air at 540 °C for 10 h.

Surface modification of MCM-41 material was achieved by a post-synthesis grafting method (Scheme 1A). One gram of calcined MCM-41 material was suspended in 50 mL of dry toluene and allowed to stir for 15 min at room temp. Then 2.5 mmol of chloropropyltrimethoxy silane (3-ClPTS) was added slowly and then the mixture was stirred overnight at reflux temperature under inert atmosphere. The material was filtered, washed with toluene, soxhlet extracted with dichloromethane (DCM) for 12 h, and then dried under vacuum. The material obtained is designated as Cl-MCM-41. The free –OH groups present in Cl-MCM-41 were protected by adding 1.5 mmol of methyltrimethoxysilane to a stirred suspension of 1 g of Cl-MCM-41 in dry toluene (50 mL), followed by stirring for 12 h at reflux temp under inert atmosphere. Then the material was filtered, washed with toluene and soxhlet extracted with DCM for 24 h. The final material was named –OH protected Cl-MCM-41 (Scheme 1B).

2.2. Synthesis of L_2Me and $L_2(Me)_2$

The L_2Me ligand was synthesized for anchoring on the solid phase and subsequent complexation with Ru and Fe, whereas the ligand $L_2(Me)_2$ was synthesized to prepare the homogeneous complexes of Ru and Fe for comparison. The following synthetic steps were adapted from the published literature (Scheme 2) for the syntheses of L_2Me and $L_2(Me)_2$ [18].

2.2.1. Synthesis of (1S,2S)-N,N′-bis(2-pyridinylmethyl)-1,2-cyclohexanediamine [L_1]

To a stirred solution of 2-pyridylcarboxaldehyde (1 g, 9.34 mmol) in methanol (25 mL), (1*S*,2*S*)-(+)-1,2-cyclohexanediamine (485 mg, 4.25 mmol) in methanol (25 mL) was added slowly under argon at 0 °C using a syringe pump. The mixture was stirred for 1 h at ambient temperature, followed by addition of anhydrous sodium sulfate, and was stirred further for another 15 min. The mixture was filtered and the solvent was removed under reduced pressure resulting in a yellow powder. It was then recrystallized from acetonitrile. Fine yellow crystals of the ligand L_1 (1.14 g, 3.9 mmol, 92% yield) were obtained.

^{1}H NMR (300 MHz, $CDCl_3$, δ (ppm)): 8.61 (d, 2H, Py, J = 4.2 Hz); 8.38 (s, 2H, C*H*=N); 7.95 (d, 2H, Py, J = 7.8 Hz); 7.71 (ddd, 2H, Py, J = 7.4 Hz); 7.29 (ddd, 2H, Py, J = 7.5, 4.3 Hz); 3.6 (m, 2H, Cy*H*N); 1.93 (m, 6H, Cy*H*); 1.65 (m, 2H, Cy*H*).

2.2.2. Synthesis of (1S,2S)-N,N′-bis(2-pyridinylmethyl)-1,2-cyclohexanediamine [L_2]

To a stirred solution of L_1 (0.3473 g, 1.19 mmol) in methanol at 0 °C was added sodium borohydride (0.1786 g, 4.76 mmol) in portions over a period of 30 min. The mixture was refluxed for 1 h, and then cooled to ambient temperature followed by addition of 2 mL of distilled water. The solvent was removed under reduced pressure leading to a white solid. The solid was dissolved in 20 mL of dichloromethane, washed successively two times with 10 mL of aqueous saturated solution of sodium bicarbonate, twice with 10 mL of distilled water and finally with 10 mL of aqueous saturated sodium chloride solution. The aqueous layer was again extracted with 10 mL of dichloromethane. The combined organic layer was slowly evaporated under reduced pressure, resulting in yellow oil L_2 (300 mg, 1.014 mmol, 85% yield).

^{1}H NMR (300 MHz, $CDCl_3$, δ (ppm)): 8.58 (d, 2H, Py, J = 5, 1.2 Hz); 7.68 (ddd, 2H, Py, J = 7.7, 1.3 Hz); 7.6 (d, 2H, Py, J = 7.7 Hz); 7.2 (ddd, 2H, Py, J = 7.7, 5 Hz); 4.1 and 3.91 (d, 2 × 2H, Ha & Hb, J = 14.09 Hz); 2.7 (s, 2H, N*H*); 2.4 (m, 2H, Cy*H*); 2.2 (m, 2H, Cy*H*); 1.77 (m, 2H, Cy*H*); 1.23 (m, 4H, Cy*H*).

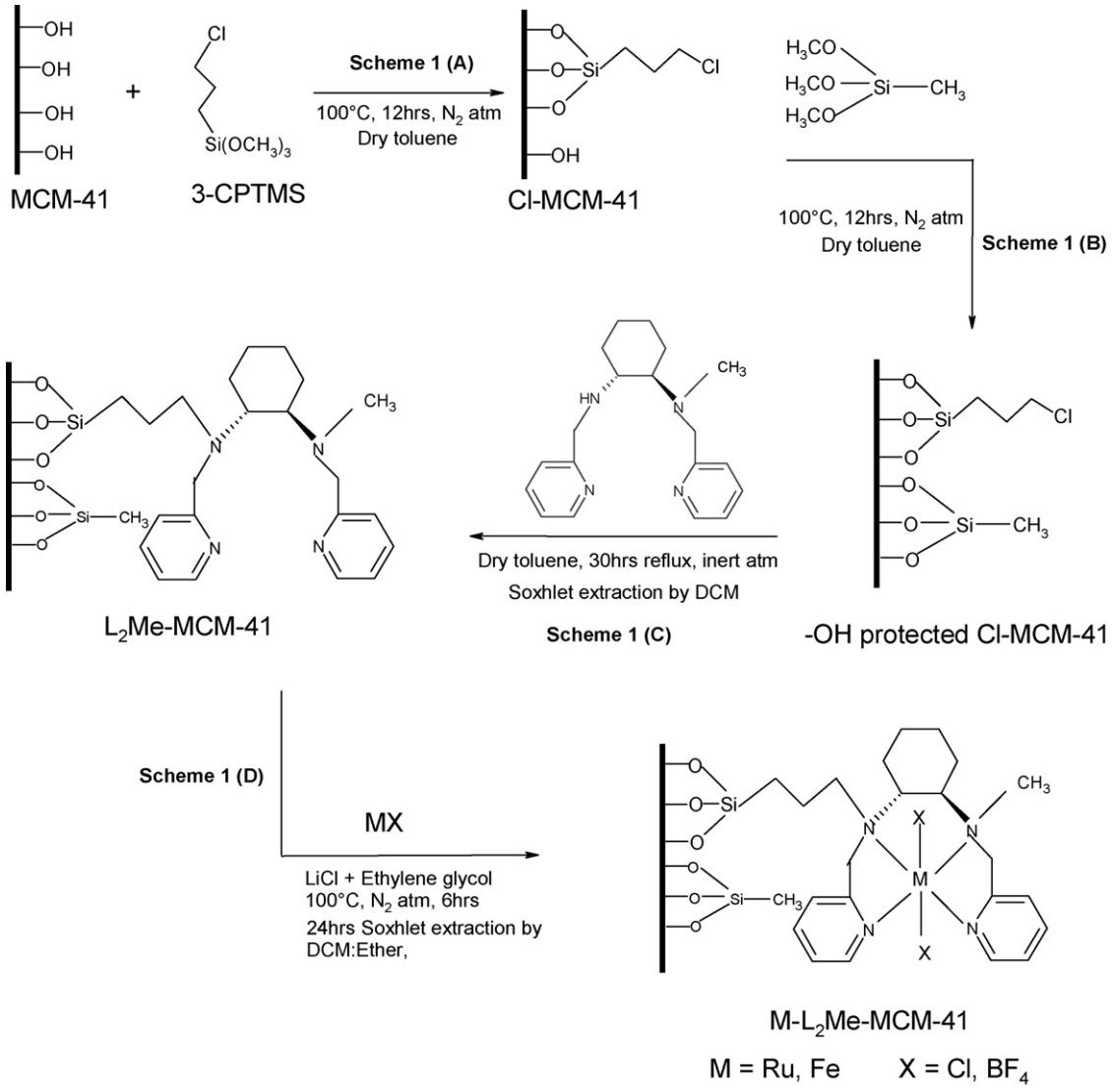

Scheme 1. Functionalization of MCM-41 and heterogenization of ligand (A) silylation of calcined MCM-41, (B) free –OH protection, (C) heterogenization of ligand and (D) metal insertion.

2.2.3. Synthesis of (1S,2S)-N-methyl-N,N′-bis(2-pyridinylmethyl)-1,2-cyclohexanediamine (L_2Me) and (1S,2S)-N,N′-dimethyl-N,N′-bis(2-pyridinylmethyl)-1,2-cyclohexanediamine [$L_2(Me)_2$]

The diamine L_2 (0.4291 g, 1.45 mmol) was dissolved in 37% formaldehyde (2.7 mL) and the resulting solution was stirred at 20 °C for 10 min. Aqueous 90% formic acid (3.3 mL) was then added and the mixture was stirred and thermally treated at 90 °C for 48 h. The mixture was then cooled to 20 °C and pH was adjusted to 12 by addition of aqueous sodium hydroxide (3 M) with constant cooling. The aqueous layer was extracted with diethyl ether (2× 50 mL) and the combined organic layers were dried (anhydrous Na_2SO_4), filtered and evaporated to give an oil, which was purified by column chromatography (Al_2O_3, ethyl acetate/hexane/triethylamine 10:4:1) to afford the title product, viz., dimethylated $L_2(Me)_2$ (0.308 g, 0.95 mmol, 66% yield) and a second product, the monomethylated L_2Me (0.122 g, 0.4 mmole, 27% yield), as clear oil.

^{1}H NMR (300 MHz, $CDCl_3$, δ (ppm))—$L_2(Me)_2$: 8.55 (d, 2H, Py, J = 4.8 Hz); 7.63 (m, 4H, Py); 7.17 (m, 2H, Py); 3.98 and 3.86 (d, 2 × 2H, CH_2, J = 14.7 Hz); 2.71 (m, 2H); 2.33 (s, 6H, 2 × CH_3); 2.02 (m, 2H); 1.81 (m, 2H); 1.26 (m, 4H), L_2Me: 8.43 (d, 2H, Py, J = 4.2 Hz); 7.56 (m, 3H, Py); 7.23 (m, 1H, Py); 7.07 (m, 2H, Py); 3.97 (d, 1H, CH_2, J = 14.1 Hz); 3.78 and 3.73 (ddd, 2H, CH_2, J = 4.5, 4.8 Hz); 3.54 (d, 1H, CH_2, J = 14.4 Hz); 2.43 (m, 2H); 2.24 (m, 1H); 2.15 (s, 3H, CH_3); 1.89 (m, 1H); 1.76 (m, 1H); 1.67 (m, 1H); 1.17 (m, 5H).

2.3. Synthesis of homogeneous complex Fe-$L_2(Me)_2(CF_3SO_3)_2$

A solution of the ligand $L_2(Me)_2$ (69 mg, 0.212 mmol) and iron triflate (93 mg, 0.212 mmol) in 15 mL of dry acetonitrile was stirred and heated under argon atmosphere for 2 h. The mixture was then cooled to ambient temperature and the solvent was removed under inert atmosphere leading to an oily residue. The residue was then treated with dry diethyl ether to give a stable,

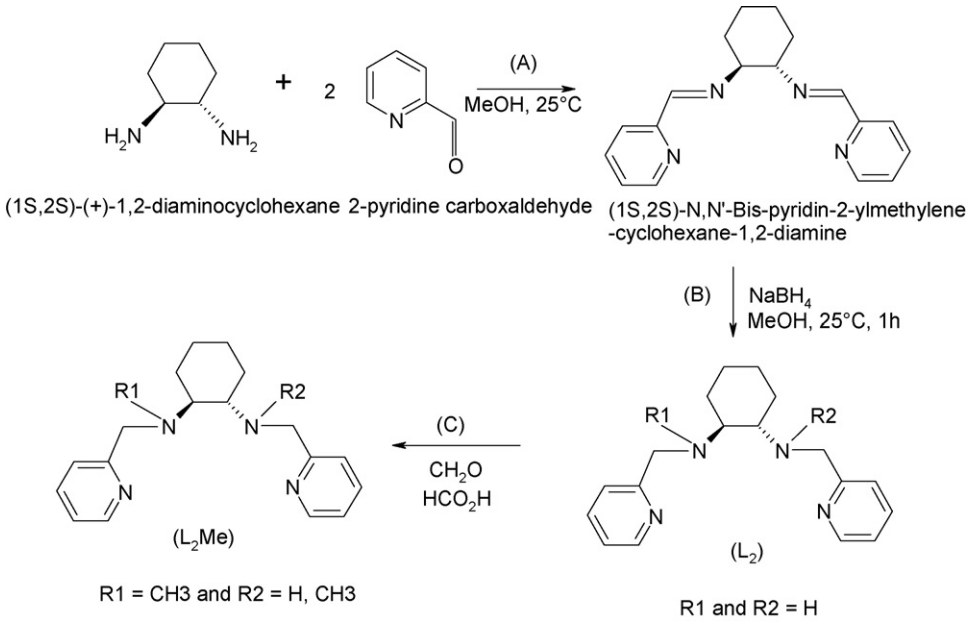

Scheme 2. Synthesis of ligand (A) synthesis of [L] (1*S*,2*S*)-*N*,*N*′-bis-pyridin-2-ylmethylene-cyclohexane-1,2-diamine, (B) synthesis of [L_2] (1*S*,2*S*)-*N*,*N*′-bis-pyridin-2-ylmethyl-cyclohexane-1,2-diamine and (C) synthesis of (1*S*,2*S*)-*N*-methyl-*N*,*N*′-bis-pyridin-2-ylmethyl-cyclohexane-1,2-diamine [L_2(Me)] or (1*S*,2*S*)-*N*,*N*′-dimethyl-*N*,*N*′-bis(2-pyridinylmethyl)-1,2-cyclohexanediamine ($L_2(Me)_2$).

brownish yellow powder of Fe-$L_2(Me)_2(CF_3SO_3)_2$ (70% yield). The complex was characterised using ^{1}H NMR and EI-MS. Data agreed with the one reported by Que and co-workers [19].

^{1}H NMR (300 MHz, CD_3CN, δ (ppm)): 106.16 (vb); 102.53 (vb); 98.31 (vb); 92.36 (vb); 88.5 (b); 76.5 (b); 53.75 (s); 51.25 (s); 48.06 (sh); 46.8 (s); 32.63 (vb); 29.66 (vb); 21.99 (vb); 17.25 (s); 8.9 (s); 7.9 (s); 6.25 (s); 5.16 (s); −3.14 (s); −12.89 (s); −31.34 (b). ESI-MS: *m*/*z* 529.3 $[L_2(Me)_2Fe(CF_3SO_3)]^+$.

2.4. Synthesis of homogeneous Ru-$L_2(Me)_2Cl_2$• DMSO

Synthesis of the ruthenium complex was adapted from a literature procedure [20]. The complex was prepared by the reaction of the ligand $L_2(Me)_2$ (50 mg, 0.17 mmol) and *trans*-$RuCl_2(DMSO)_4$ (81 mg, 0.17 mmol) in toluene (10 mL) at 110 °C for 22 h. The formed precipitate was filtered and was recrystallized from acetone by ether diffusion leading to a green powder (40 mg, 70 μmol, 75% yield).

^{1}H NMR (300 MHz, CD_2Cl_2, δ (ppm)): 9.1–9.3 (m, Py-H); 8.25 (d, Py-H); 7.3–8.0 (m, Py-H); 4.9 (d, CH_2); 4.7 (d, CH_2); 4.3–4.45 (m, CH_2); 3.1–3.6 (m); 3.4 (s, 2N-CH_3); 2.15–2.9 (m); 1.5–2.0 (m); 1.2 (t). ESI-MS: *m*/*z* 539.1 $[L_2(Me)_2RuCl(DMSO)]^+$, 461.31 $[L_2(Me)_2RuCl]^+$. UV–vis [λ_{max}, nm (ε, M^{-1} cm^{-1}) in CH_2Cl_2]: 639 (1058); 476 (1054); 362 (4078); 246 (6564).

2.5. Grafting of (1S,2S)-N,N′-bis-pyridin-2-ylmethyl-cyclohexane-1, 2-diamine (L_2Me) ligand inside the Cl-MCM-41

The ligand, L_2Me, was introduced into the inner surfaces of MCM-41 by adding a solution of 0.1 g of L_2Me in 10 mL of dry CH_2Cl_2 to a stirred suspension of –OH protected Cl-MCM-41 (1 g) in dry toluene (30 mL). This mixture was refluxed for 24 h in inert atmosphere, filtered, and washed with toluene and then with CH_2Cl_2 followed by soxhlet extraction, with 1:1 mixture of DCM:diethyl ether for about 24 h. The final material is called as L_2Me-MCM-41 (Scheme 1C). The final proportion of the anchored ligand over Cl-MCM-41 is 7 wt.% of the solid.

2.6. Complexation of Ru and Fe in the L_2Me-MCM-41

2.6.1. Complexation of Ru with L_2Me-MCM-41

Ruthenium was inserted into the L_2Me moiety by adding 1 g of L_2Me-MCM-41 to a stirred solution of 0.2 g of $RuCl_3{\cdot}3H_2O$ and 0.22 g of LiCl in of ethylene glycol (15 mL). The mixture was heated to about 110 °C for about 6 h in inert condition and soxhlet extracted with 1:1 mixture of ethanol:ether. The final yellow green material was called Ru-L_2Me-MCM-41.

2.6.2. Complexation of Fe with L_2Me-MCM-41

Iron was inserted into the L_2Me moiety by adding 1 g of L_2Me-MCM-41 to a stirred solution of 0.2 g of Fe $(BF_4)_2$ in a Schlenk tube under argon atmosphere at room temperature. The mixture was stirred for 2 h and the solvent was then removed. The resulting lightly yellow powder was washed with methanol until the solution was totally colourless. The final material was called Fe-L_2Me-MCM-41.

2.7. Reactivity: oxidation of sulfide catalyzed by Fe(II) and Ru(II) complexes

Oxidation reactions were carried out in a 5 mL flask equipped with a magnetic stirrer. The flask was charged with 3 mL of a solution or suspension of the catalyst (0.007 mmol) in methanol and stirred for 15 min, and then methyl phenyl sulfide (1 mmol)

and the oxidant (2.5 mmol of 30% H_2O_2 or PhIO or TBHP) were added under stirring. An internal standard (20 μL of a 1 M solution of benzophenone in acetonitrile) was added to the reaction mixture. Chemical yield and enantiomeric excess were measured by GC/MS.

3. Characterization of the catalysts

Synthesized catalysts were characterized by X-ray diffraction using a Rigaku Miniflex powder diffractometer on finely powdered samples using Cu Kα radiation and 45 kV 40 mA. The XRD patterns were recorded for 2θ between 1.5° and 10°, at a scan rate of 2°/min. Adsorption of nitrogen was carried out at 77 K using a NOVA 1200 (Quantachrome) apparatus for analyzing surface areas and pore-size distributions of the synthesized catalysts. Specific surface areas were calculated following the BET procedure. Pore-size distribution was obtained by using the BJH pore analysis applied to the desorption branch of the nitrogen adsorption/desorption isotherms. FT-IR spectra of solid samples were taken in the range of 4000–400 cm^{-1} on a Shimadzu FT-IR 8201 instrument. Thermogravimetric analyses (TGA and DTA) were performed using a Diamond TG/DTA instrument, from 30 to 1000 °C at a heating rate of 10 °C/min under airflow. Ruthenium and iron contents in the catalysts were determined using a GBC Avanta Ver 1.32 AAS instrument. Analyses of the organic content present in the catalysts were carried out using a Carlo-Erba C, H, and N analyzer. UV–vis spectra were recorded by a JASCO spectrometer equipped with a diffuse reflectance attachment, using $BaSO_4$ as the reference. The scanning electron microscope (SEM) photographs of the samples were obtained using a JEOL-JSM-5200 instrument. XPS of the samples were recorded using a VG Microtech multilab ESCA 3000 spectrometer equipped with a twin anode of Al and Mg. All the measurements were made on as-received powder samples using Mg Kα X-ray at room temperature. Base pressure in the analysis chamber was 4×10^{-10} Torr. A Multichannel detection system with nine channels was employed to collect the data. The overall energy resolution of the instrument was better than 0.7 eV, determined from the full width at half-maximum of the $4f_{7/2}$ core level of a gold surface. The errors in all BE values were within ±0.1 eV. Surface analysis by XPS spectra was carried out in terms of the binding energy (BE) values of various elements present in the catalyst supports after necessary C 1s correction, which was the major element in our system. EPR experiments at 4 K were performed with a Band X Bruker EMX 300 equipped with an OXFORD cryostat. Solution 300 MHz ^1H NMR spectra were recorded on a DPX300 Brüker spectrometer.

Gas chromatography (GC) equipped with a MS detector was performed on a Perkin-Elmer Autosystem XL instrument, using a SE 30 column. Enantiomeric excess were measured using a Chiral capillary column Lipodex-E.

4. Results and discussion

4.1. X-ray diffraction (XRD)

Fig. 1 shows the powder X-ray diffraction (XRD) patterns of calcined MCM-41, OH protected Cl-MCM-41, Ru-L_2Me-MCM-41 and Fe-L_2Me-MCM-41 materials. The typical hexagonal phase of MCM-41 [main (1 0 0) peak with weak (1 1 0), (2 0 0), and (2 1 0) reflections] is clearly visible in calcined MCM-41 [21]. Due to partial loss of space correlation of the pores, the reflection almost disappeared (indices 2 1 0) after the post-synthesis modification. This kind of resultant disorder in the silica mesostructure has been commonly observed in the studies of silylation of the mesoporous silicas. However, the retention of the characteristic peaks [(1 0 0), (1 1 0) and (2 0 0)] indicates that the mesostructure is retained after incorporation of organic functional groups, ligand and metals. Moreover, a slight decrease in the peak intensities was observed in the case of the metal complex loaded samples, which might be due to partial filling of the void space due to the presence of metal complexes inside the mesopores. A comparison of unit cell parameter (a_0) values (calculated from XRD patterns) of the functionalized MCM-41 and those with anchored metal complexes is presented in Table 1.

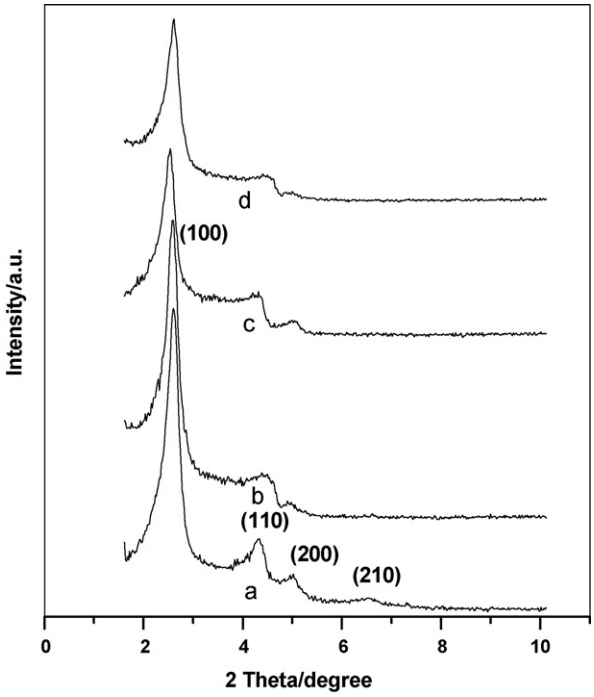

Fig. 1. XRD patterns of (a) calcined MCM-41, (b) –OH protected Cl-MCM-41, (c) Ru-L_2Me-MCM-41 and (d) Fe-L_2Me-MCM-41.

4.2. FT-IR spectra

Fig. 2 shows the FT-IR spectra of the as-synthesized, calcined, and –OH protected Cl-MCM-41, the neat ligand (L_2Me), Fe-L_2Me-MCM-41 and Ru-L_2Me-MCM-41. The strong and broad band in the region of 3600–3200 cm^{-1} corresponds to the hydrogen bonded Si–OH groups present in the mesoporous samples and a sharp peak at 3743 cm^{-1} corresponds to the free silanol group [22]. All the MCM-41 samples, except calcined MCM-41, show bands in the region of 2800–2900 cm^{-1} corresponding to the C–H stretching frequency of the surfactant in the case of as-synthesized MCM-41, chloropropyltrimethoxy and methyl-

Table 1
Summary of the catalyst properties

Sample	Metal (wt.%)	a_0[a] (Å)	Pore diameter (Å)	Pore volume ($cm^3\ g^{-1}$)	S_{BET} ($m^2\ g^{-1}$)
Calcined MCM-41	–	41.6	31.1	0.8	1082
Cl-MCM-41	–	40.4	31.0	0.7	1019
–OH protected Cl-MCM-41	–	41.1	30.1	0.5	696
Ru-L_2Me-MCM-41[b]	1.71	42.5	31.0	0.5	615
Fe-L_2Me-MCM-41[c]	1.95	41.8	28.6	0.4	585

[a] Unit cell parameter (a_0) = $d_{100} \times 2\sqrt{3}$.
[b] Ligand grafted Cl-MCM-41; elemental analysis: C = 8.8%, H = 2.1%, N = 1.2% and Ru = 1.71% (from AAS analysis). Input ligand grafted on Cl-MCM-41 = 10 wt.%; output of ligand grafted on Cl-MCM-41 = 7 wt.%.
[c] Ligand grafted Cl-MCM-41; elemental analysis: C = 9.8%, H = 2.3%, N = 1.3% and Fe = 1.95% (from AAS analysis).

triethoxy groups in the case of –OH protected Cl-MCM-41 and with the ligand moiety in the case of Fe-L_2Me-MCM-41 and Ru-L_2Me-MCM-41. The band at 1080 and 800 cm^{-1} is assigned to the asymmetric and symmetric Si–O–Si vibrations of MCM-41, respectively, and the band at 970 cm^{-1} is assigned to the asymmetric Si–OH vibration [23]. The IR spectrum of the neat ligand L_2Me shows C–H stretching bands in the region of 3020–2855 cm^{-1} and a sharp C–N stretching vibration of tertiary amine at 1218 cm^{-1}. The band between the regions 1430–1665 cm^{-1} corresponds to the ring stretching vibration of the ligand. The C=N stretching band of the heterocyclic ring appears along with the C=C band near 1592 cm^{-1} [24]. However, in the heterogenised catalyst because of low loading of ligand all the major characteristic bands (C–N and C=N bands) were overlapped with the Si–O–Si stretching bands of mesoporous material (Fig. 2e and f) and are hardly indiscernible.

4.3. Nitrogen sorption studies

Incorporation or anchoring of organic groups or metal in the framework position and/or into the wall of mesoporous materials usually results in a progressive decrease in their surface area [25,26]. N_2 sorption studies of all catalysts exhibited type IV behavior, characteristics of mesoporous material [27,28] according to the IUPAC classification. The BET surface area, pore volume and pore diameter of all catalysts are shown in Table 1. The decrease in surface area and pore volume of functionalized MCM-41 is attributed to the functionalization of organic moieties onto mesoporous wall. Before the functionalization, the position of inflection in the P/P_0 = 0.2–0.4 region depends on the diameter of the mesopores and its moderate sharpness indicates the uniformity of the pore size distributions (Fig. 3A). After the functionalization with chloropropyltrimethoxysilane the position of inflection is in the P/P_0 = 0.2–0.4 region Fig. 3B. The pore size distribution curve of metal complex grafted catalysts shows one small extra pore corresponds to the less ordered structure. The position of inflection (P/P_0) is also changed considerably (shown in Fig. 3C and D). These results indicate that the mesoporosity of MCM-41 samples was decreasing during each treatment, which may be attributed to the anchoring of various moieties on the inner pore walls of MCM-41.

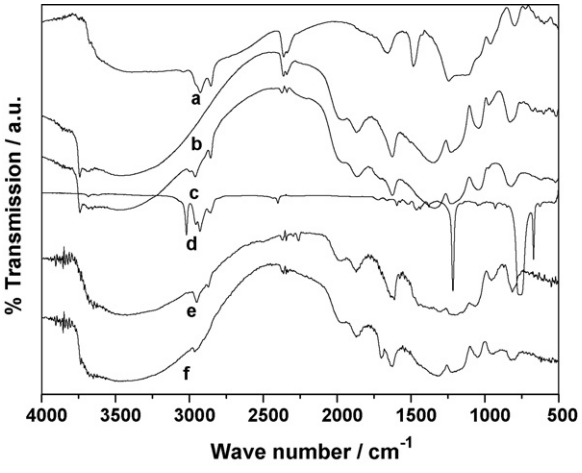

Fig. 2. FT-IR spectrum of the (a) as synthesized, (b) calcined, (c) –OH protected Cl-MCM-41, (d) neat ligand, (e) Ru-L_2Me-MCM-41 and (f) Fe-L_2Me-MCM-41.

4.4. Thermal analysis

Fig. 4 shows the TGA–DTG pattern of as-synthesized, calcined, and –OH protected Cl-MCM-41, the neat ligand (L_2Me), Ru-L_2Me-MCM-41 and Fe-L_2Me-MCM-41. The TGA curve of as-synthesized MCM-41 sample shows three peaks for weight loss. The first weight loss (endothermic) below 150 °C corresponds to the loss of physisorbed water molecule. The significant second weight loss that occurred in the region 150–380 °C is attributed to the removal of surfactant in the as-synthesized MCM-41 [11,29]. Moreover, a small weight loss in the range of 600–800 °C corresponds to the dehydration of the hydroxyl groups inside the pores (Fig. 4a).

In the case of calcined MCM-41, we observed only two weight losses corresponding to physisorbed water molecule (below 150 °C) and dehydration of the hydroxyl groups inside the pores (around 650 °C), indicating that all the surfactant molecules are removed during the calcination process (Fig. 4b). Along with the above (calcined MCM-41) weight losses, we observed an additional third weight loss in the case of –OH protected Cl-MCM-41 in the range between 250 and 300 °C, which could correspond to the removal of 3-CPTMS and methyltrimethoxysilane (Fig. 4c). For the neat ligand there is only one weight loss in the range of 250–300 °C (Fig. 4d), which is shifted to 460–600 °C in the case of Ru/Fe-L_2Me-MCM-41

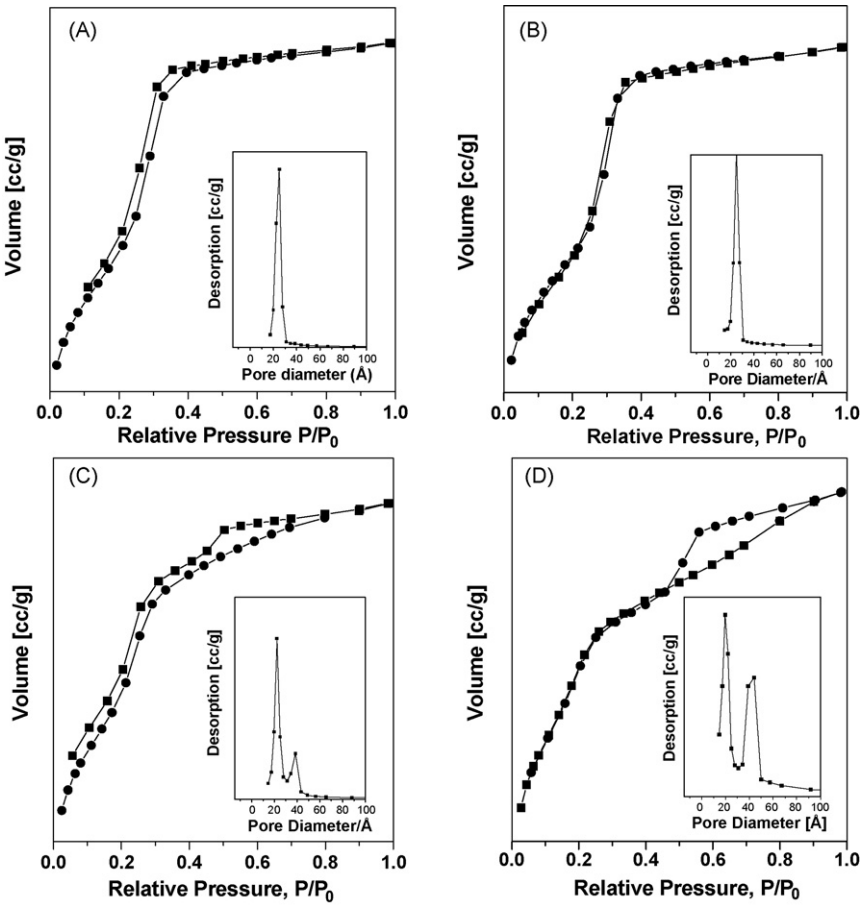

Fig. 3. Nitrogen adsorption–desorption isotherms and pore-size distribution (inset) of (A) calcined, (B) Cl-MCM-41, (C) Ru-L_2Me-MCM-41 and (D) Fe-L_2Me-MCM-41.

catalysts, indicating that the heterogenized metal complexes are more stable than the pure ligand (Fig. 4e and f). These results are confirmed by the comparison of DTG pattern of –OH protected Cl-MCM-41 with that of Ru/Fe-L_2Me-MCM-41, which shows additional weight loss in the range of 460–600 °C, due to removal of heterogenized metal complex. The DTA pattern further supports the above findings as it shows the strong exothermic peak around 400 °C and around 550 °C. All these results clearly indicate the successful grafting of organic moieties, as well as metal complexes inside the mesoporous channels.

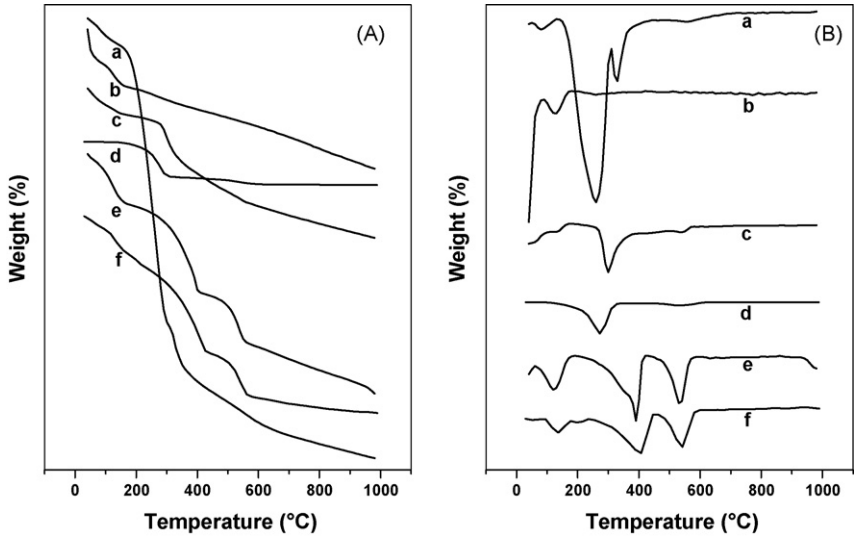

Fig. 4. TGA (A)–DTG (B) pattern of (a) as synthesized, (b) calcined, (c) –OH protected Cl-MCM-41, (d) neat ligand, (e) Ru-L_2Me-MCM-41 and (f) Fe-L_2Me-MCM-41.

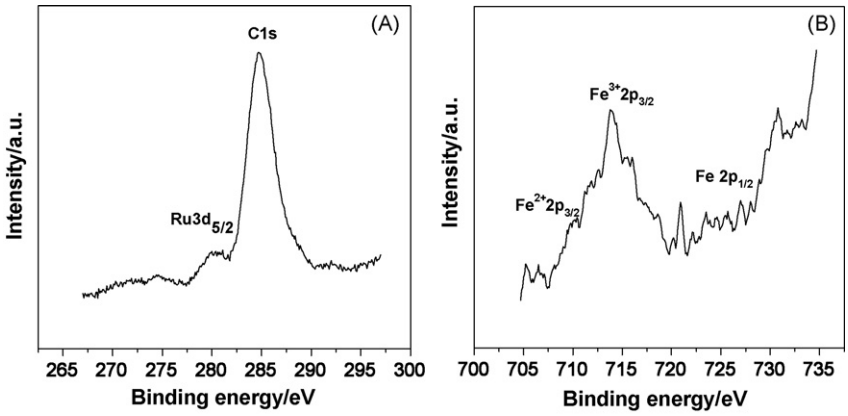

Fig. 5. XPS spectrum of (a) Ru-L_2Me-MCM-41 and (b) Fe-L_2Me-MCM-41.

4.5. X-ray photoelectron spectra (XPS)

Additional support for anchoring of Ru ^{II} complexes onto the solid mesoporous material was obtained by the XPS study. In XPS ruthenium $3d_{5/2}$, $3d_{3/2}$ and $3p_{3/2}$ peaks are observed at 280.6, 284.4 and 464.9 eV, respectively, which confirm that ruthenium is present in the Ru^{II} state [30]. The N 1s binding energy (BE) of 400.8 and 399.8 eV of ligand grafted catalysts (Ru/Fe-L_2Me-MCM-41, respectively) indicates successful grafting of the complex; however shifting in the BE were observed in each case, which can be attributed to the coordination of N atom to Ru and Fe nuclei and also confirmed the presence of heterogenized ligand in the MCM-41. All these results strongly point to stable anchoring of the metal complexes onto the mesoporous support. The absence of Ru^{III} was also corroborated by the absence of any signal in the X band EPR signal.

The XPS spectrum of Fe-L_2Me-MCM-41 reveals a major binding energy values at 713.8 eV and a minor one at 709.8 eV, in agreement with the presence of Fe^{III} and Fe^{II}, respectively (Fig. 5B). The presence of high spin Fe^{III} was confirmed by the presence of a signal at $g = 4.3$ in the X band EPR (figure not shown).

4.6. ^{13}C CP/MAS NMR study

Fig. 6 shows the liquid state ^{13}C NMR spectrum of 3-CPTMS (spectrum A) and $L_2(Me)_2$ (spectrum B), and the high resolution solid state ^{13}C CP/MAS NMR spectra of Cl-MCM-41 (spectrum C) and L_2Me-MCM-41 (spectrum D). The liquid state ^{13}C NMR of 3-CPTMS shows four distinct peaks [C1 (attached with silicon), C2, C3 (attached with chlorine) and methoxy carbon at 6.6, 26.12, 47.17 and 50.39 ppm, respectively]. After

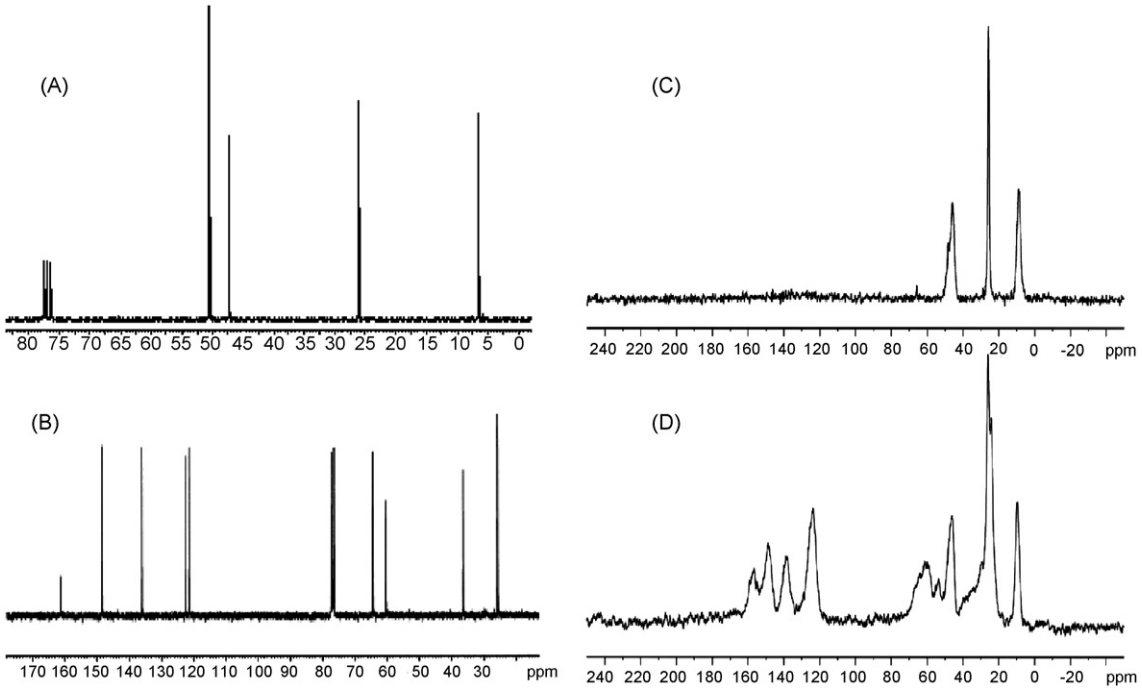

Fig. 6. Liquid state (A and B) ^{13}C NMR and solid state (C and D) ^{13}C CP/MAS NMR spectrum of (A) 3-CPTMS, (B) pure ligand $L_2(Me)_2$, (C) Cl-MCM-41 and (D) L_2Me-MCM-41.

grafting of 3-CPTMS on MCM-41, the entire peaks broaden and shift to lower field (10.29, 26.34 and 47.99 ppm, respectively) corresponding to carbon C1–C3, respectively, and no peak was observed for the methoxy group, which confirms the successful grafting of 3-CPTMS onto the support (spectrum C). The grafting of the L_2Me ligand is confirmed by the presence of new resonances in the ^{13}C CP/MAS NMR spectrum in addition to the ones observed in spectrum C. First, in the 180–120 ppm region, four peaks are observed attributed to ^{13}C resonances of carbons of the pyridyl rings, in a range similar to the ones observed in the liquid spectrum of L_2Me. Moreover, in the region 0–60 ppm, in addition to the resonances of C1–C3 of the propyl linker, two resonances are attributed to the methylene carbon of the cyclohexane ring (shoulder at 25 and 28 ppm) and the broad ones above 50 ppm concerns the resonances of the methylene group and the C–H of the ligand. The attributions were based on simulation using ACD/CNMR Predictor software (http://www.acdlabs.com/products/spec_lab/predict_nmr/cnmr/).

Metallation of the ligand with iron was demonstrated by the absence of pyridine resonances and the slight shifts of the propyl resonances, attributed to the paramagnetism of the metal (data not shown).

Thus, the ligand was found grafted into the phase and metallated. The absence of any other resonances suggests that most of the chloropropyl groups have reacted with the amino group of the ligand.

4.7. Diffuse reflectance UV–vis spectra

The UV–vis/DRS spectra of the samples were essential for a proper understanding of the nature of the metal species, especially supporting and complementing previous characterization data of these materials. Fig. 7 shows the UV–vis spectra of the pure MCM-41, Ru-L_2Me-MCM-41 and Fe-L_2Me-MCM-41. The absorption above 40,000 cm^{-1} corresponds to the siliceous materials (Fig. 7a). The absorption spectrum of Ru-L_2Me-MCM-41 shows at least three metal-to-ligand charge transfer (MLCT) absorption bands at 15,917, 20,341 and 26,517 cm^{-1} (Fig. 7b) [31,32]. The band in the UV region at 32,957 cm^{-1} is assigned to an intra ligand (π–π^*) transition which is also observed for Fe-L_2Me-MCM-41. Absorption at 38,174 cm^{-1} is typically assigned to Fe^{3+} species, either tetrahedrally coordinated or with higher coordination (Fig. 7c) [33,34]. Because of very low amount, we could not observe peaks corresponding to the Fe^{2+} species (which is supported by XPS and EPR). Generally d–d transitions of Fe^{3+} species are expected in the range of 30,000–15,500 cm^{-1}, but they are symmetric and spin-forbidden, and therefore extremely weak [34]. All these results support XPS and EPR findings.

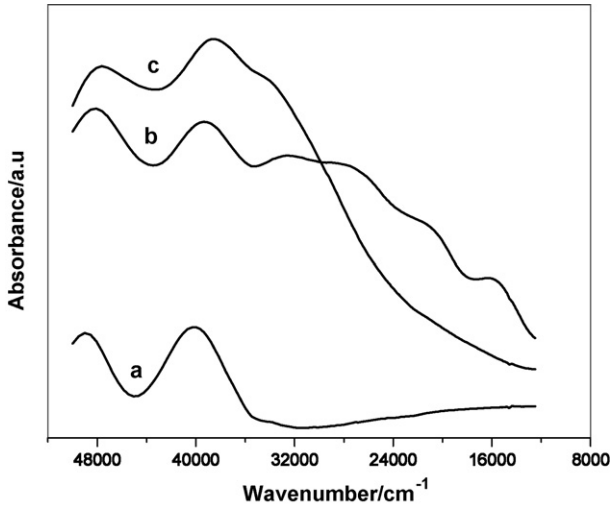

Fig. 7. DR UV–vis spectra of (a) pure MCM-41, (b) Ru-L_2Me-MCM-41 and (c) Fe-L_2Me-MCM-41.

4.8. Scanning electron microscopy (SEM)

The scanning electron micrographs show the particle morphology of before and after modifications of the MCM-41 samples. The SEM image of calcined, –OH protected Cl-MCM-41, Ru-L_2Me-MCM-41 and Fe-L_2Me-MCM-41 samples are shown in Fig. 8. All the four micrographs show considerable differences in the morphology of the mesopore after grafting of each organic moiety. Calcined MCM-41 shows the hexagonal structure uniform in particle size. The uniformity of the particle size gets reduced after the grafting of various organic moieties on the inner pore walls of MCM-41, indicating that various treatment conditions can affect the morphology of MCM-41.

4.9. Catalytic activity

Structural characterization results show that the metal complexes are firmly held inside the pore channels of mesoporous MCM-41. Hence, the present materials were applied in the liquid phase sulfoxidation of methyl phenyl sulfide with H_2O_2 as the oxidant at room temperature. All the experiments were performed with a catalyst:substrate:oxidant ratio of 1:100:250.

The results obtained after 4.5 h from the sulfoxidation reaction over neat (Fe-L_2(Me)$_2$, Ru-L_2(Me)$_2$) complexes as well as immobilized complexes (M-L_2Me-MCM-41) are presented in Table 2 and were compared with those obtained from anchored MCM-41 (L_2Me-MCM-41) and without catalyst are also included for comparison. Furthermore, the influence of reaction time, catalyst amount in the case of M-L_2Me-MCM-41 and different oxidizing agents such as H_2O_2, PhIO and TBHP in the case of Ru-L_2Me-MCM-41 are examined on the conversion of methyl phenyl sulfide, TON, and selectivity to the methyl phenyl sulfoxide.

From Table 2, it is clear that mesoporous MCM-41 functionalized metal complexes show an enhanced activity (in terms of conversion of methyl phenyl sulfide and turnover number, TON) compared to the L_2Me-MCM-41 solid phase and in the absence of catalyst. Moreover, the selectivity towards the sulfoxide (sulfoxide/sulfone + sulfoxide) over all catalysts was found between 81 and 92%, a greater value than the one of the uncatalyzed reaction (70%).

The conversion of methyl phenyl sulfide reached 100 and 90% over Ru-L_2Me-MCM-41 and Fe-L_2Me-MCM-41 after 1.1

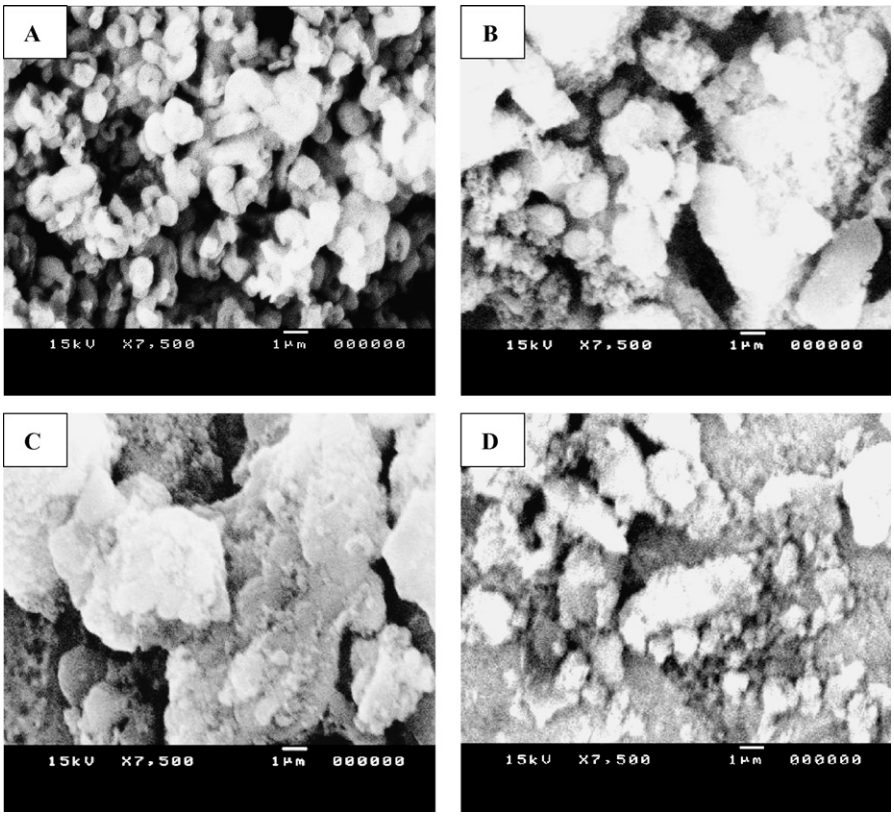

Fig. 8. SEM image of (A) calcined MCM-41, (B) –OH protected Cl-MCM-41, (C) Ru-L_2Me-MCM-41 and (D) Fe-L_2Me-MCM-41.

and 6 h, respectively, when 100 mg of the catalyst amount was used instead of 50 mg.

The reaction efficiency of the solid catalysts was found to be metal dependent. The conversion of methyl phenyl sulfide as a function of reaction time over Ru-L_2Me-MCM-41, Fe-L_2Me-MCM-41 and without catalyst are given in Fig. 9. Ru-L_2Me-MCM-41 showed considerably superior performance throughout the reaction and it gave about 100% conversion of methyl phenyl sulfide in 4 h, whereas Fe-L_2Me-MCM-41 gave up to 75% conversion level in 5.5 h of reaction time.

Table 2
Oxidation of methyl phenyl sulfide promoted by supported Ru and Fe catalysts

Catalysts	%Conversion (time, h)	Selectivity to sulfoxide (%)	TON[a]
No catalyst	23 (4.5)	70	–
L_2Me-MCM-41	16 (4.5)	85	–
Ru-L_2Me-MCM-41	98 (4.5)	90	90
Fe-L_2Me-MCM-41	75 (4.5)	81	50
Fe-$L_2(Me)_2$[b]	100[c] (5 min)	36	42
Ru-$L_2(Me)_2$[d]	95 (5 min)	93	82
Ru-L_2Me-MCM-41 (100 mg)	100 (1.1)	88	46
Fe-L_2Me-MCM-41 (100 mg)	90 (6)	80	41
Ru-L_2Me-MCM-41	35 (4.15)[e]	92	31
	20 (4)[f]	86	17

Reaction conditions: catalyst amount = 50 mg; methyl phenyl sulfide = 1 mmol; H_2O_2 (30%) = 2.5 mmol; methanol = 3 mL; reaction temperature = room temperature.

[a] TON = (mmol of sulfoxide + mmol of sulfone)/mmol of Ru or ligand grafted.

[b] To be changed by amount of Ru/Fe-$L_2(Me)_2$ corresponding to concentration of iron complex in supported catalysts (i.e. 1% moles vs. substrate).

[c] Mass balance was under 100% revealing the presence of undefined products.

[d] Amount of Ru/$L_2(Me)_2$ taken.

[e] Oxidation with PhIO.

[f] Oxidation with TBHP.

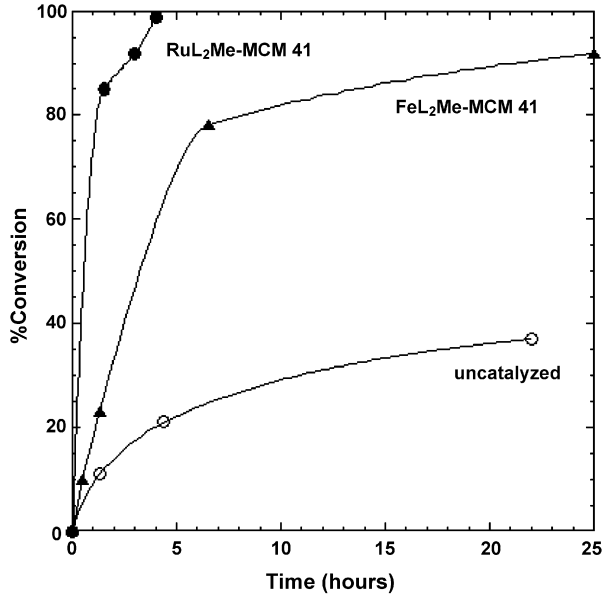

Fig. 9. Conversion of methyl phenyl sulfide (%) vs. reaction time over various catalysts; reaction conditions as in footnote of Table 2.

Interestingly, the heterogenization of metal complex caused remarkable changes as the reactivity was concerned. First, homogeneous Fe-$L_2(Me)_2(CF_3SO_3)_2$ led to a less selective sulfoxidation than its grafted counterpart. In the homogeneous case, 100% conversion was attained in 5 min with only 36% of sulfoxide, but other products coming from a *S*-dealkylation were formed. Then, the grafting of Fe-L_2(Me) on MCM-41 led to a different reaction pathway, which led to a neat selective oxygen transfer reaction. Second, the reaction time of the sulfoxidation was greatly increased when the MCM-41 support was present (5 min against 4–10 h). This strongly suggests that the reaction took place in the pores where the presence of oxidant and substrate are regulated by the pore size. Third, the grafting of Ru($L_2(Me)_2$)Cl_2 initiates an enantioselective reaction (7%), whereas only the racemic mixture was formed in homogeneous catalysis. It has to be noted that the grafting of Fe-L_2Me did not alter its asymmetric efficiency (2%).

Finally, the influence of various oxidizing agents, such as H_2O_2, PhIO and TBHP was also observed in the sulfoxidation of methyl phenyl sulfide using the Ru-L_2Me-MCM-41 catalyst. The H_2O_2 gave higher conversion (98%) compared to the PhIO (35%) and TBHP (20%). However, no significant changes were observed in the selectivity of sulfoxide (Table 2).

The catalytic properties of the both heterogeneous catalysts unambiguously support that the L_2Me ligand is entered into the pores, leading to high selectivity and good efficiency.

Furthermore, the epoxidation of styrene was also carried out over Fe-L_2Me-MCM-41 for 26 h at 70 °C in DMF using H_2O_2 as an oxidant. The ratio of catalyst:substrate:oxidant was kept: 1:135:135. The main products of the reaction were benzaldehyde and styrene epoxide. The results were also compared with the homogeneous catalyst, Fe-$L_2(Me)_2$, and in the absence of catalyst under the similar reaction conditions except setting the reaction time at 6 h. The conversion of styrene, selectivity to styrene epoxide and TON over Fe-L_2Me-MCM-41 and Fe-$L_2(Me)_2$ were found to be 42, 75, 39 and 32, 82 and 33%, respectively. In this case, no major difference was observed regarding the efficiency of the two catalysts. In the absence of catalyst, no epoxide was detected in the epoxidation of styrene.

No color changes have been observed during the reaction, excluding any characterization of transient intermediates. On the other hand, literature reports over the homogeneous catalyst Fe-$L_2(Me)_2$ [35] reveal that a high valent iron species was responsible for alkane and alkene oxidation. We may suggest that in the case of sulfoxidation either a peroxo adduct of the complex or an oxene species is involved in the oxidation process.

4.10. Recycling studies

In order to ascertain whether the activity of the immobilized catalysts arise from true heterogeneous catalysts, the stability of the metal complexes over MCM-41 (Ru-L_2Me-MCM-41, Fe-L_2Me-MCM-41) were tested three times (fresh + two cycles) in the sulfoxidation of methyl phenyl sulfide using H_2O_2 as an oxidant. The results are presented in Table 3. After workup of reaction mixture, the catalyst was separated by filtration, washed three times with methanol and dried in vacuum before use in the next experiment. The recovered catalyst after each reaction was analyzed for the nitrogen content to see the amount of complex leached out from the solid phase. Elemental analysis showed that the N_2 content from Ru-L_2Me-MCM-41 and Fe-L_2Me-MCM-41 decreased from 0. 41 to 0.21 and 1.1 to 0.25%, respectively, after use from fresh to second recycle, respectively. Similarly, the conversion of methyl phenyl sulfide decreased from 97 to 70 and 92 to 72% when Ru-L_2Me-MCM-41 and Fe-L_2Me-MCM-41 were recycled from fresh to the second cycle, respectively. However, the selectivity to the methyl phenyl sulfoxide did not change appreciably after each recycling. The loss of metal complex by leaching from the mesoporous MCM-41 phase is responsible for the slight decrease in catalytic activity of both catalysts after each recycle.

Table 3
Recycling of M-L_2Me-MCM-41 catalysts in phenyl methyl sulfide reaction

	Conversion (%)	Selectivity	%N content
Ru-L_2Me-MCM-41[a]			
Fresh	98	90	0.41
Recycle I	71	70	–
Recycle II	70	96	0.21
Fe-L_2Me-MCM-41[b]			
Fresh	92	87	1.10
Recycle I	82	80	–
Recycle II	72	94	0.25

Reaction conditions as in footnote of Table 2; see Section 2, for the recycling conditions.
[a] Reaction time = 4.5 h.
[b] Reaction time = 23 h.

5. Conclusions

Iron and ruthenium complexes were successfully grafted on to MCM-41 support which was modified by 3-CPTMS. The resulting materials were subjected to the different characterization techniques, such as XRD, FT-IR, TG-DTA, UV–vis, solid state ^{13}C NMR and EPR, which reveal that the metal complexes are firmly attached to the modified MCM-41 support. The screening of the catalysts, Ru/Fe-L_2Me-MCM-41, was done in the sulfoxidation reaction of thioanisole using H_2O_2 as an oxidant. It has been indicated that the heterogenized metal complexes (Ru/Fe-L_2Me-MCM-41) plays an important role in the sulfoxidation of thioanisole, which give higher activity, TON and selectivity compared to the homogeneous counterpart. During recycling, conversion of methyl phenyl sulfide decreases from 98 to 90 and 92 to 72% after use from fresh to second recycle over Ru-L_2Me-MCM-41 and Fe-L_2Me-MCM-41, respectively. Furthermore, Fe-L_2Me-MCM-41 and Fe-$L_2(Me)_2$ were also found active in the epoxidation of styrene.

We are currently investigating new catalytic properties of these heterogeneous systems and modification of the polynitrogen ligands in our laboratory in order to improve the enantioselectivity (ee) of the sulfoxidation.

Acknowledgments

We are grateful to the IFCPAR (Indo-French Centre for the Promotion of Advanced Research) for a collaborative grant (3105-D). We thank C. Lebrun (CEA-Grenoble, DRFMC, SCIB) and G. Gerbaud (CEA-Grenoble, DRFMC, SCIB, LRM) for ESI-MS and solid-state NMR analyses, respectively.

References

[1] D.E. De Vos, M. Dams, B.F. Sels, P.A. Jacobs, Chem. Rev. 102 (2002) 3615.
[2] (a) K. Neimann, R. Neumann, A. Rabion, R.M. Buchanan, R.H. Fish, Inorg. Chem. 38 (1999) 3575;
(b) W.A. Carvalho, M. Wallau, U. Schchardt, J. Mol. Catal. A: Chem. 144 (1999) 91.
[3] (a) F. Fache, E. Schulz, M. Lorraine Tommasino, M. Lemaire, Chem. Rev. 100 (2000) 2159;
(b) L. Canali, D.C. Sherrington, Chem. Soc. Rev. 28 (1999) 85;
(c) V. Schünemann, A.X. Trautwein, I.M.C. Rietjens, M.G. Boersma, C. Veeger, D. Mandon, R. Weiss, K. Bahl, C. Colapitro, M. Piech, R.N. Austin, Inorg. Chem. 38 (1999) 4901 (and references therein).
[4] (a) M. Fontecave, S. Ménage, C. Duboc-Toia, Coord. Chem. Rev. 178–180 (1998) 1555;
(b) M. Costas, K. Chen, L. Que Jr., Coord. Chem. Rev. 200–202 (2000) 517 (and references therein).
[5] M. Costas, A.K. Tipton, K. Chen, D.-H. Jo, L. Que Jr., J. Am. Chem. Soc. 123 (2001) 6722.
[6] (a) J. Legros, C. Bolm, Angew. Chem. Int. Ed. 43 (2004) 4225;
(b) Y. Mekmouche, H. Hummel, R.Y.N. Ho, L. Que Jr., V. Schuenemann, F. Thomas, A.X. Trautwein, C. Lebrun, K. Gorgy, J.C. Lepretre, M.-N. Collomb, A. Deronzier, M. Fontecave, S. Menage, Chem. Eur. J. 8 (2002) 1196.
[7] C.T. Kresge, M.E. Leonowicz, W.J. Roth, J.C. Vartuli, J.S. Beck, Nature 359 (1992) 710.
[8] J.S. Beck, J.C. Vartuli, W.J. Roth, M.E. Leonowicz, C.T. Kresge, K.D. Schmitt, C.T.W. Chu, D.H. Olson, E.E. Sheppard, S.B. McCullen, J.B. Higgins, J.L. Schlenker, J. Am. Chem. Soc. 114 (1992) 10834.
[9] A. Corma, M.T. Navarro, J.P. Pariente, J. Chem. Soc. Chem. Commun. (1994) 147.
[10] P.T. Tanev, M. Chibwe, T.J. Pinnavaia, Nature 368 (1994) 321.
[11] S. Shylesh, A.P. Singh, J. Catal. 228 (2004) 333.
[12] D. Brunel, A. Cauvel, F. Fajula, F. DiRenzo, in: L. Bonneviot, et al. (Eds.), Studies in Surface Science and Catalysis, vol. 97, Elsevier, Amsterdam, 1995, pp. 173–180.
[13] J.J. Diaz, K.J. Balkus Jr., F. Bedioui, V. Kurshev, L. Kevan, Chem. Mater. 9 (1997) 61–67.
[14] C.W. Jones, K. Tsuji, M.E. Davis, Nature 393 (1998) 52–54.
[15] T. Asefa, M.J. Maelachlan, N. Coombs, G.A. Ozin, Nature 402 (1999) 867.
[16] S. Inagaki, S. Guan, Y. Fukushima, T. Ohsuna, O. Terasaki, J. Am. Chem. Soc. 121 (1999) 9611.
[17] R.J.P. Corriu, D. Leclereq, Angew. Chem. 108 (1996) 1524.
[18] A.J.A. Cobb, C.M. Marson, Tetrahedron 61 (2005) 1269–1279.
[19] M. Costas, J.-U. Rohde, A. Stubna, R.Y.N. Ho, L. Quaroni, E. Munck, L. Que Jr., J. Am. Chem. Soc. 123 (2001) 12931.
[20] J.-X. Gao, T. Ikariya, R. Noyori, et al., Organometallics 15 (1996) 151087–151089.
[21] A. Ghosh, R. Kumar, J. Catal. 228 (2004) 386.
[22] J. Chen, Q. Li, R. Xu, F. Xiao, Angew. Chem. Int. Ed. Engl. 34 (1995) 2694.
[23] M.D. Alba, Z. Luan, J. Klinowski, J. Phys. Chem. 100 (1996) 2178.
[24] C.J. Pouchert, The Aldrich Library of Infrared Spectra, 3rd ed., p. 1305.
[25] A.N. Parvulescu, B.C. Gagea, M. Alifanti, V. Parvulescu, V.I. Parvlescu, S. Nae, A. Razus, G. Poncelet, P. Grange, J. Catal. 202 (2001) 319.
[26] N.C. Marziano, L.D. Ronchin, C. Tortato, A. Zingales, A.A. Sheikh-Osman, J. Mol. Catal. A: Chem. 174 (2001) 265.
[27] M.J. Hudson, J.A. Knowles, J. Mater. Chem. 6 (1996) 89.
[28] M. Schneider, A. Baikar, J. Mater. Chem. 5 (1992) 587.
[29] S.C. Laha, P. Mukherjee, S.R. Sainkar, R. Kumar, J. Catal. 207 (2002) 1.
[30] C. Battistoni, C. Furlani, G. Mattogno, G. Tom, Inorg. Chim. Acta 21 (1977) L25.
[31] T.R. Weaver, T.J. Meyer, S.A. Adeyemi, G.M. Brown, R.P. Eckberg, W.E. Hatfield, E.C. Johnson, R.W. Murray, D. Untereker, J. Am. Chem. Soc. 97 (1975) 3039.
[32] Md.K. Nazeeruddin, S.M. Zakeeruddin, R. Humphry-Baker, S.I. Gorelsky, A.B.P. Lever, M. Gratzel, Coord. Chem. Rev. 208 (2000) 213.
[33] S. Bordiga, R. Buzzoni, F. Geobaldo, C. Lamberti, E. Giamello, A. Zecchina, G. Leofanti, G. Petrini, G. Tozzolo, G. Vlaic, J. Catal. 158 (1996) 486.
[34] A. Bruckner, R. Luck, W. Wieker, B. Fahlke, H. Mehner, Zeolites 12 (1992) 380.
[35] K. Chen, L. Que Jr., J. Am. Chem. Soc. 123 (2001) 6327.